



Corrosion of carbon steel in formic acid as an organic pollutant under the influence of concentration cell

Suzan T. Abbas, Basim O. Hasan

Department of Chemical Engineering, Al-Nahrain University, Iraq

Corresponding Author E-mail: basimohasan13@gmail.com

Abstract:

The presence of contaminants in water even in small amounts can cause considerable corrosion damages of metals. This is due to free corrosion effect or the formation of concentration cell of pollutants resulting in a galvanic effect. The current work was devoted to study the effect of formic acid (CH_2O_2) as an organic pollutant on the corrosion rate of carbon steel under different operating conditions. It includes an investigation of galvanic corrosion caused by the establishment of concentration cell of formic acid under different operating conditions. The ranges of operating parameters were formic acid concentration of 10^{-4} - 10^{-5} M and temperature of 32 - 50 °C. The results showed that increasing formic acid concentration to 10^{-4} M leads to an increase in the corrosion rate by up to 7.6 times that in the water of 0.1N NaCl. In addition, the corrosion rate in each terminal in concentration cell also increased by up to 2.3 times. Pumping of air in formic acid solution led to a considerable increase in the corrosion rates and enhances the concentration cell effect which increases the galvanic currents. High increase of corrosion rate was noticed by pumping the air at high temperature reaching up to 4 times depending on temperature. In general, the galvanic currents were high initially and decreased with time due to the formation of corrosion product layer. The increase in temperature from 25 to 50 °C caused an increase in the galvanic corrosion rate reached up to 2 times in formic acid solution. In addition, the galvanic currents were noticed to decrease with temperature while the corrosion rate of each terminal was increased.

Keywords: corrosion, carbon steel, concentration cell, formic acid, aeration solution, temperature.

1. Introduction:

Carbon steel is the major metal from which the equipment in petroleum industry and other industries are made. Corrosion can attack this metal due to the presence of corrosive organic or inorganic material in the solutions [1]. Acid rain normally contains organic acids such as formic acids, acetic acid, and benzoic acid that causes effective corrosion problem to a variety steel structures in used in petroleum refineries like underground pipelines, tanks, and other processing equipment. These rains contact the steel structures by direct contact or by soil acidification. Also, it causes a considerable corrosion damage on the buried metals. Soil is the receives large amount of acid rain normal, thus a different of changes occur due to the effect of the acid rain. The soil becomes acidified when the amounts of acid rain becomes larger than buffer capacity [2]. The effect of corrosion on structures due to the presence of acid in most areas is mainly local nature. However, acidification of soil and water may cause to increase corrosion of buried structures, including water pipes. Besides, there is a common problem in the first place, where the long-range transport of existed pollutants in air have a considerable influence. The metal corrosion due to atmosphere resulting from acid deposition is often a local problem appears in areas close to the source of contamination. The main reason of this type of corrosion is the dry deposition of air pollutants. The elevated gases from industrial plants dissolve in the rain to form acid rain. The corrosion effect of acid rain is depending on the materials and on the amounts of contamination [2]. Galvanic corrosion is one of the most common types of corrosion, resulting from two metals connected by a conductor in a corrosive medium. Galvanic corrosion occurs also when a certain metal is exposed to a concentration difference of some specific corrosive species what so called concentration cells [1]. The rates of galvanic corrosion and the potential difference over a galvanic couple terminals are dependent on the electrochemical properties of the metals, and environmental variables such as oxygen content, temperature, salts concentration, solution properties, and flow rate. In addition to that the corroding system geometry, a larger flexibility in the material selection may be possible if dissimilar materials can be coupled without significant damage [3]. The presence of some kinds of pollutants in the water or liquids with which an industrial equipment deals can cause an appreciable corrosion rate which is influenced by process conditions such as temperature and flow rate. In this context, different pollutants

are possible to be present in water. Formic acid is a weak organic acid and slow to react causing a considerable corrosion damage for a long term of exposure. However, it is more difficult to control formic acid corrosion at the elevated temperatures [4]. Oxygen plays an important key in corrosion process but it is not usually presented in the dissolved liquids. At the drilling stage, oxygenated liquids are injected for the first time. The drilling mud may cause corrosion of the casing of wells, drilling equipment, pipelines, and the equipment of mud handling. The aim of present work is to investigate the effect of formic acid as an organic pollutant on the corrosion rate of carbon steel especially when establishing the concentration cell of formic acid on carbon steel metal under different process conditions.

2. Experimental Work:

Corrosion of carbon steel was investigated in a formic acid containing solution. The chemical composition of the carbon steel under study as shown in Table 1. The experimental work presented here involved three parts. Firstly, the corrosion of carbon steel specimen was determined as a free corrosion test in formic acid of different concentrations that were: 10^{-4} , 10^{-5} , and 10^{-7} M. Secondly, concentration cell experiments were carried out by connecting different concentrations of formic acid with 0.1N NaCl solution to determine the corrosion rates in this case. Therefore, in concentration cell experiments the electrolytes were two separated solutions on contains polluted solution with formic acid CH_2O_2 concentration and the other was 0.1N NaCl solution. Thirdly the formic acid solution is aerated by pumping air at different temperatures of 32 °C and 50 °C.

Table (1) Chemical analysis of carbon steel specimens.

Component	Mg	Al	Si	P	S	Ti	V	Cr
(Wt. %)	0.020	0.0044	0.0016	0.00098	0.0020	0.0016	0.0014	0.1248
component	Mn	Co	Ni	Cu	Zn	As	Zr	Nb
(Wt. %)	0.472	0.425	0.0022	0.0519	0.0060	0.00017	0.013	0.0037
Component	Mo	Ag	Cd	Sn	Sb	W	Pb	Fe
(Wt. %)	0.183	0.00061	0.00063	0.00099	0.0010	0.0042	0.0012	97.73

The salt used was pure NaCl. The formic acid used was purchased from the local market with a molecular weight of 46.03 g/g mole and density of 1.22 g/cm³. The distilled water used in experiments with a conductivity of 6.63 μ S, pH of 6.86, oxygen solubility of 6.08 ppm at laboratory temperature 27 °C. Ethanol was used to clean the specimens. It was supplied by FLUKA with a assay of 99.9 %. The specimens were cut into coupons of dimensions 40 × 40 mm. One side of the specimen was exposed to the solution while other was completely insulated, thus the total surface area of 1600 mm². The specimens were holed from the center by fine screw for the purpose of holding it in the solution. The area of hole was very small and negligible compared to the total exposed area of the specimen. The concentration cell was formed by connecting two beakers of different formic concentrations with salt bridge as shown in Figure (1). Before each test, the electrode specimens were abraded with emery paper of different grades: 120, 220, 400, and 2000. Then, they were washed with brushing using plastic brush in running tap water to remove part of the corrosion products. After that it is washed by distilled water, dried using clean tissue, followed by immersion in ethanol for 30 s. Then using electrical oven at about 80 °C for 3 minute [5,6] The specimens were stored in a desiccator over high activity silica gel until use.

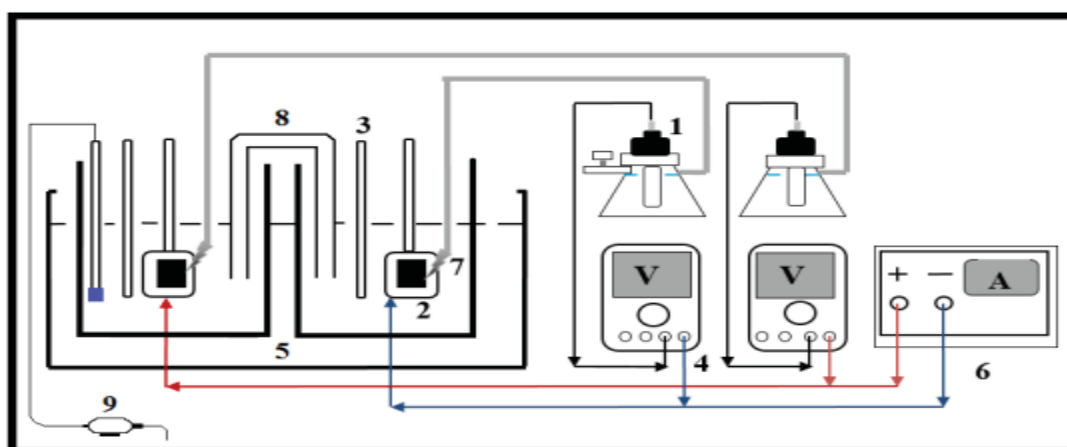


Fig. (1): Experimental apparatus: 1- Calomel Electrode (Reference Electrode), 2- Specimens, 3-Thermometer, 4- Voltmeter, 5- Water Bath, 6- Zero Resistance Ammeter (ZRA), 7- Luggin Capillary, 8- Salt Bridge, 9- Air Pump.

The specimens were weighted by accurate balance to obtain their weights before corrosion test. After the solution reached the required temperature, the two specimens were electrically connected by a wire to measure galvanic currents variation with time by using Zero Resistance Ammeter (ZRA) where one specimen was connected to the (+ve) and the other to the (-ve) terminal. The coupon was mounted by connecting it on holding board using a fine screw. The effect of the screw was ignored. During each experimental run, galvanic potential variation with time was measurement by using Standard Calomel Electrode SCE bridged. The galvanic current and galvanic potential of the couple specimens were measured for 2 hours immersion time in the solution. After each test, the specimens were weighted by highly sensitive balance of accuracy 0.1 mg (SAUTER type). The corrosion rate for two similar metals calculated in gmd by:

$$CR = \Delta W / A \times t \quad (1)$$

Where ΔW the weight loss in gram, A is the area in m^2 , and t is the time in day.

3. Results and Discussion:

3.1 Corrosion Potentials

Figures 2 and 3 show the free corrosion potential (OCP) versus time for carbon steel for solution of 0.1N NaCl and 10^{-4} M CH_2O_2 respectively at different temperatures. It was noticed from Figure (2) that the beginning of the run a high corrosion potential is found decayed quickly with time. This potential decay is due to the oxide film formation on the metal surface and due to the reduction in surface activity. After the immersion this film undergoes reductive dissolution and the corrosion potential decreases with time reaching the asymptotic value [7]. It can also be seen that the corrosion potential shifts to more negative values with increasing temperature. This is due to the escape of O_2 from the solution as shown in Table (2). This is in agreement with [8]. In Figure (3) at 25 °C and the OCP exhibits a potential shift to more negative. The reduction in potential over time is due to continuous corrosion [9]. The initial reduction of OCP is because a partial dissolution of the formed film followed by the posterior passivation film growth [10, 11]. The anodic iron dissolution in formic acid solution produces hydrated ferrous ions. The metallic iron dissolves in the form of hydrated ferric ions which means that the passive film is mainly ferric oxide, Fe_2O_3 as in the following equations [12]:



These two reactions occur simultaneously causing the passive layer at a constant thickness, which increases with the increase in the anodic potential. Table 3 lists the corrosion rate in gram per square meter per day (gmd) of C.S. specimen in 0.1 N NaCl only and in CH₂O₂ solutions of concentrations of 10⁻⁴, 10^{-4.5}, 10⁻⁵, and 10^{-5.5} M CH₂O₂ at (25, 32, 40, and 50) °C for 2 h of immersion time.

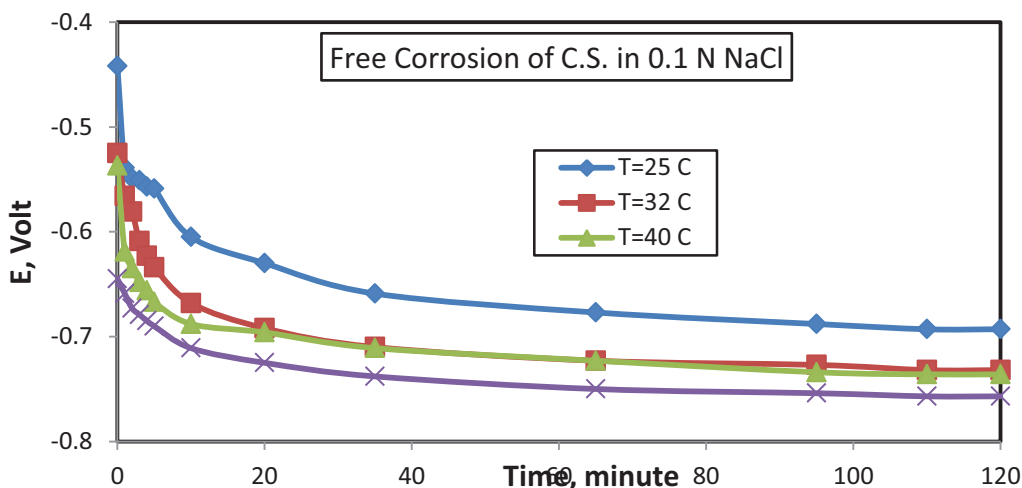


Fig. (2) Corrosion potential vs. time of C.S. in 0.1 N NaCl at different temperatures.

Table (2) Oxygen solubility at atmospheric pressure [13].

T, °C	30	35	40	45	50	55	60
Solubility (mg/l) in 0.1 N NaCl	7.5	6.9	4.3	5.3	5.9	4.4	

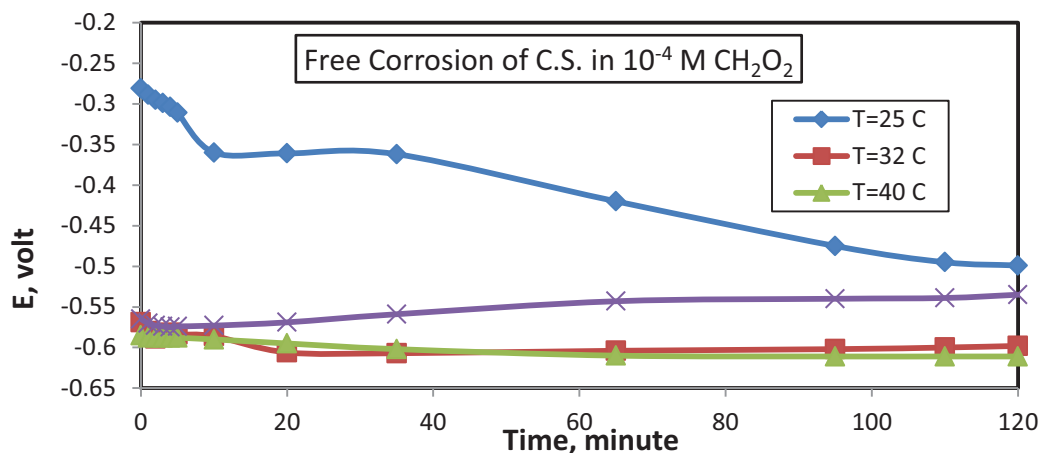


Fig. (3) Corrosion potential vs. time of C.S. in 10^{-4} M of CH_2O_2 at different temperatures.

Table3: Corrosion rate of carbon steel at different formic acid concentrations and different temperatures.

CR, gmd				
Concentration of formic acid, M	25 °C	32 °C	40 °C	50 °C
0.1N NaCl solution	10.5	11.1	14.2	15.9
$10^{-5.5}$	—	30.3	—	—
10^{-5}	—	63.5	—	—
$10^{-4.5}$	—	72.8	—	—
10^{-4}	67.1	84.3	116.0	234.8

From Table (3), it is clear that the corrosion rate increases with increasing temperature especially in the case of formic acid. The temperature effect on the corrosion rate is represented by changing two parameters that are the O_2 diffusivity and O_2 solubility. Increasing the temperature reduces the viscosity of the aqueous solutions, which causes an increase in the rate of oxygen diffusion to the surface of the metal and thus increase the rate of corrosion [14, 15, 23]. On the other hand, the oxygen solubility decreases with increase temperature. Increasing temperatures leads to an increase in hydrogen ion diffusivity and promote the reaction kinetic on hydrogen ion reduction on the metal surface the factor that enhances the corrosion [5, 16]. In addition, Table 3 indicates the rate of corrosion increases with increasing in acid concentration. The study of Osarolube et al. [17] stated that the

corrosion of mild steels in acid solutions was attributed to the presence of oxygen, and H^+ which accelerated the corrosion process.

3.2 Galvanic Corrosion (Concentration Cell Corrosion)

Figures (4 and 5) show the potential of CS couple of each specimen in different solutions (Sp.1 in formic acid solution and the Sp.2 in 0.1N NaCl solution). From these Figures, it can be observed due to the galvanic effect of concentration difference, the potential of Sp.1 shifts slightly toward the noble (positive) direction and Sp.2 toward the active (negative) direction. Accordingly, since Sp.1 potential is less negative than the Sp.2 potential, therefore, it will behave as the anode in the galvanic couple, while Sp.2 would be a cathode.

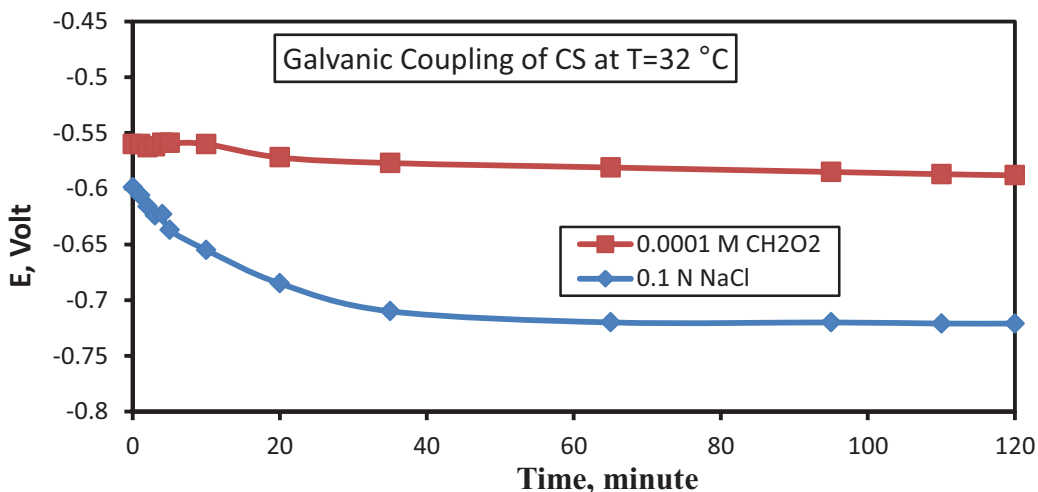


Fig. (4) Potential vs. time of C.S. couple in 0.1N NaCl with 10^{-4} M CH₂O₂ and T=32 °C.

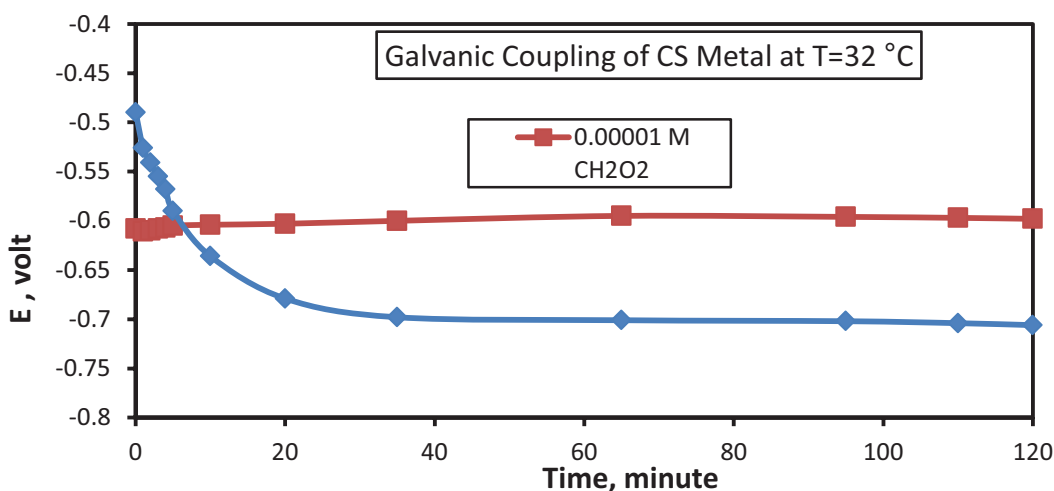


Fig. (5) Potential vs. time of C.S. couple in 0.1N NaCl with 10^{-5} M CH₂O₂ and T=32 °C.

3.2.1 Effect of Temperature

Figures (6 and 7) show the effect of temperature on potential of CS couple in 0.1N NaCl and 10^{-5} M CH_2O_2 respectively. The temperature also has an effect on the solubility of air in the water. Generally, one can see a trend that the high temperatures have a lower redox potential. This seems reasonable since the increased temperature increases the kinetic energy of the oxygen molecules which increases the possibility for them to leave the solution. This is in agreement with previous works [18, 24]. From Figure 6, it is evident that the potential at $T= 40$ °C and 50 °C after 5 and 10 minutes respectively is shifting towards positive values and became higher than at $T=32$ °C. Then it becomes lower than $T=32$ °C after 90 and 45 minutes respectively. While, , it can be seen from Figure (7) that the potential of $T= 25$ °C and 32 °C is shifting towards positive values and then starts decreasing after 80 minutes opposite than in $T= 40$ and 50 °C is shifting towards the negative values and in $T= 50$ °C was higher than in 40 °C until reaching the steady state value of -0.636 V for 95 minutes. In addition, one can see that the highest potential is at $T= 32$ °C. The galvanic current estimated by the use ZRA, where the Sp.1 (CH_2O_2 solution) is connected to the positive terminal of the ZRA and the Sp.2 (NaCl solution) is connected to the negative terminal. Figure (8) shows the galvanic current of the CS couple versus time in different temperatures for 0.1N NaCl with 10^{-5} M CH_2O_2 solution. At $T=32$ °C, the galvanic current increases in first 15 minutes to reach the steady value. At $T=40$ °C, there is a clear increase in galvanic current over time to reach the maximum value of 13 μA at 75 minutes. Then, the current decreases slightly with time. The current increases to 6.9 μA at 30 minutes and then decreases sharply until it is established about 0.1 μA . Also, it increases to 0.7 μA at the 15 minutes, and then decreases to 0.5 μA for 10 minutes and increases slightly again over time at $T=25$ °C.

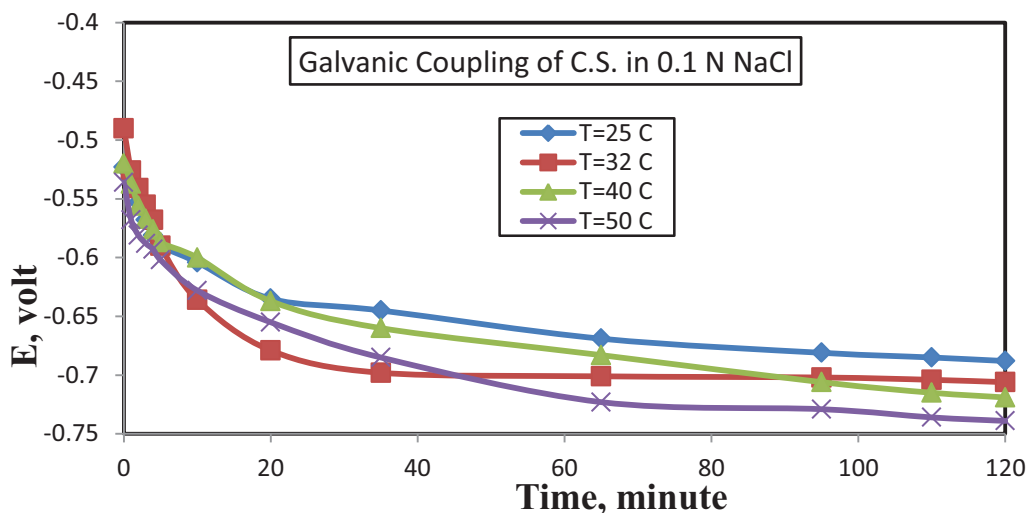


Fig. (6) Potential vs. time of CS couple in 0.1 N NaCl and different temperatures.

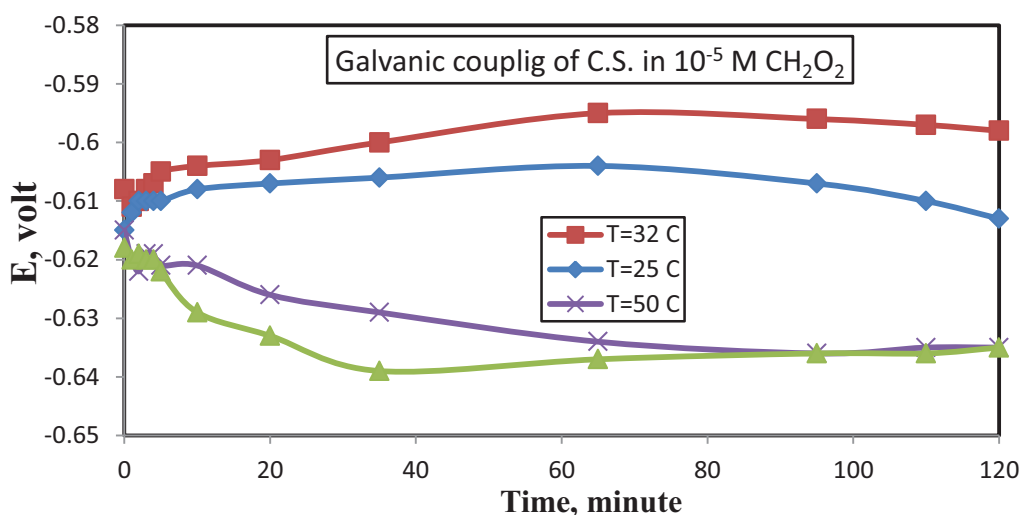


Fig. (7) Potential vs. time of CS couple in 10^{-5} M CH_2O_2 and different temperatures.

The maximum value is apparently dependent on the temperature. It can be seen that at highest temperature (50 °C) the current is lowest. This is attributed to the low oxygen solubility [14]. At the beginning, the metal surface is active which causes higher corrosion rate. As the process time proceeds, a corrosion product layer starts to form on the surface which leads to a decrease in the activity of the metal surfaces and restrains the diffusion of oxygen to the surface and thus the galvanic corrosion decreases. The higher the temperature and the higher the galvanic current are needed, but this difference decreases with time.

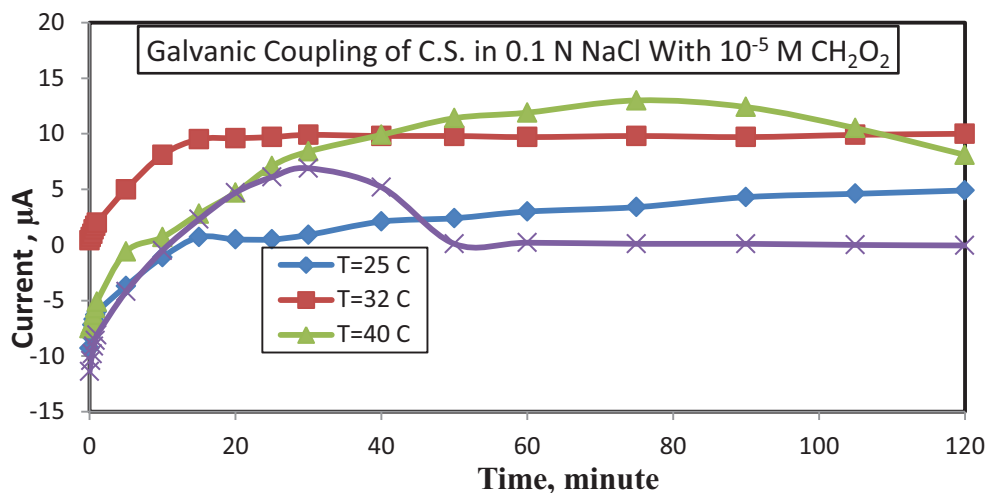


Fig. (8) Galvanic current vs. time for CS couple in 0.1N NaCl with 10⁻⁵ M CH₂O₂ and different temperatures.

3.2.2 Effect of Pollutants Concentration

Figure (9) shows a comparison of acid concentration on potential of CS couple in T=32 °C. As seen from Figure (9) that as acid concentration increases, the potential increases (becomes more positive). The behavior is attributed to the fact that increasing acid concentration at the interface between metal and solution leads to increase the rate of reaction for metal dissolution [14].



Figure (10) illustrates the variation of corrosion rate of CS specimens expressed in gmd with temperature coupled where Sp. 2 in salt coupled to Sp. 1 in acid solutions. The values of corrosion rate reveal that the corrosion rate of SP.2 in 0.1N NaCl is lower than that for SP.1 in 10⁻⁵ M CH₂O₂. This indicates cathodic reactions in NaCl compartment is domination while in the acid compartment the anodic reaction dominant. During the galvanic corrosion, the reactions occurring in salt side as shown below:

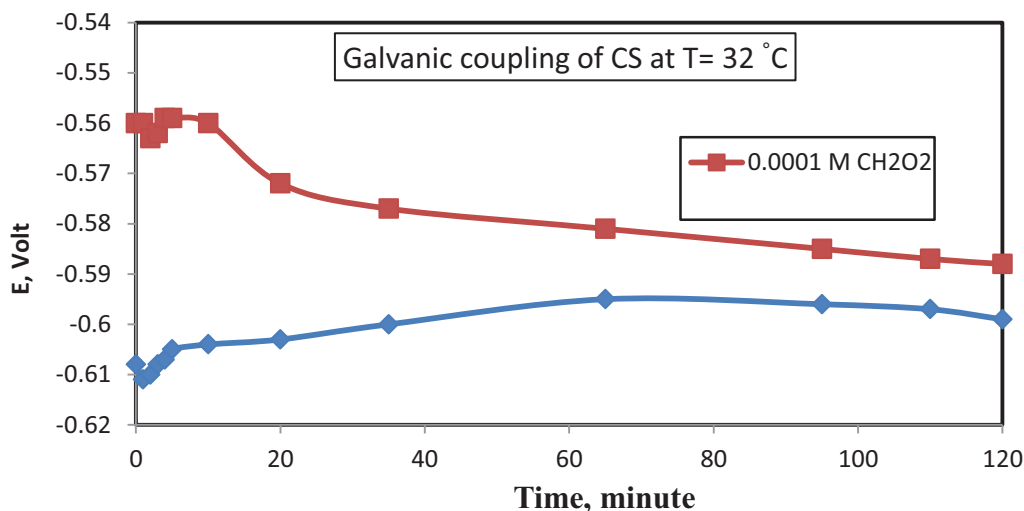
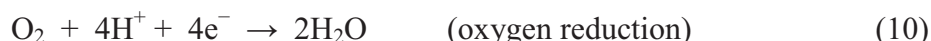
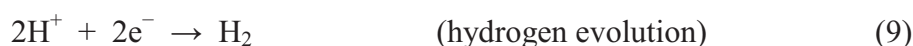
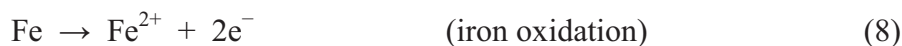


Fig. (9) Potential vs. time of C.S. couple in different acid concentrations and T=32 °C.

Equations (6) to (10) are the anodic and cathodic reactions occurring on both specimens:



And in the acid side:



These reactions occur in both free and galvanic cases. In case of galvanic coupling, the anodic reaction in acid solution at Sp.1 decreases, i.e. the iron dissolution due to the influence of lower potential Sp.2 in NaCl solution which shift the potential of Sp.1 to more negative causing partial cathodic protection of Sp.1. However, the anodic reactions (iron dissolution) in NaCl solution also increases as the Sp.2 increases. For both specimens, there is an equivalent increase or decrease in the cathodic reaction of oxygen reduction and hydrogen evolution to balance the total current. Corrosion rate shows considerably increase in salt-acid solution compared with solution containing salt only. The presence of acid in the salt solution makes the process under mixed control, i.e. mass transfer and activation control. In addition, the mixture becomes more corrosive and the corrosion rate in 10^{-5} M CH_2O_2 is higher than that in salt solution alone. The increase in the corrosion rate of CS leading to the increase in the acid concentration (i.e. the corrosion rate in 10^{-4} M CH_2O_2 is

74.233 and it decreases to 37.1 in 10^{-5} M CH_2O_2 at same temperature) due to the increase in evolution of hydrogen reaction which causes a greater metal surface dissolution [19]. The temperature increase of acidic solutions influences the corrosion rate of materials in several ways: (i) it increases the rate of electrochemical reaction. As the system in current work is under kinetic (activation) control, the increase in temperature is very influential [20], (ii) The temperature increases causes an increase in the solubility of the reaction products which may results in different corrosion reactions (iii) viscosity decreases which causes an increase in the oxygen diffusivity [21,22].

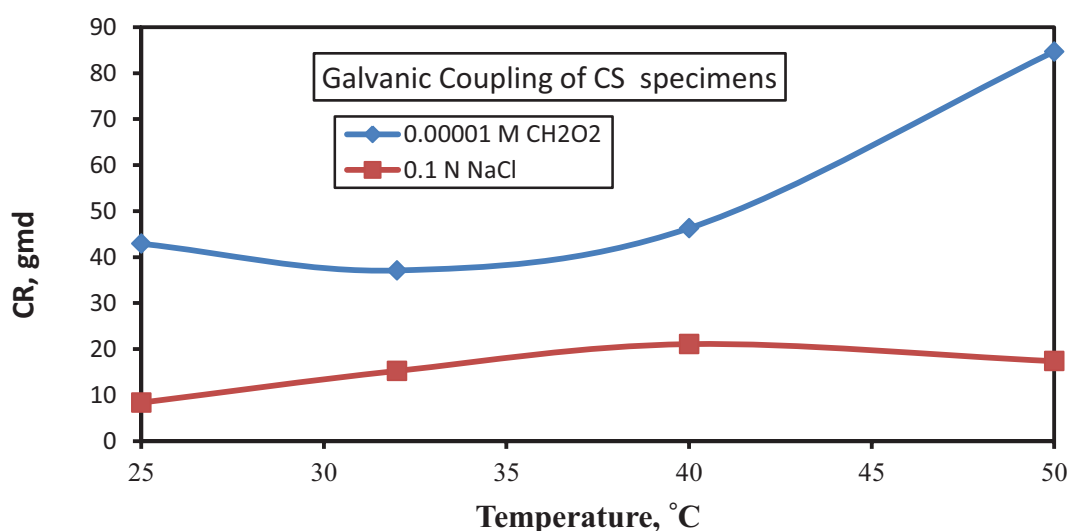


Fig. (10) Variation of corrosion rate of CS couple with temperature in 0.1N NaCl and 10^{-5} M CH_2O_2 solution.

Table (4) lists the corrosion rate of CS couple in gmd in 0.1N NaCl only and 0.1N NaCl connected to 10^{-4} M and 10^{-5} M CH_2O_2 at T= 25, 32, 40 and 50 °C. The values of corrosion rate reveals that the corrosion rate of Sp.1 is higher than that for Sp.2 and which indicates the Sp.1 is anodic and Sp.2 is cathodic in the galvanic couple. Comparing Table 4 for concentration cell coupling with Table 3 for free corrosion indicates that:

1. The CR of Sp. 2 immersed in 0.1N NaCl solution in case of galvanic coupling is higher than the case of free corrosion. The CR in case of coupling with 10^{-4} M is higher by 2.3 times than in the case of free corrosion in 0.1NaCl solution. This is due the effect of high potential acid solution coupled to 0.1N NaCl solution.

2. The free CR of Sp. 1 in acid solution is decreased when coupling it with Sp.2 in 0.1N
3. NaCl solution. This is due to the effect of lower potential 0.1N NaCl solution.
4. The corrosion rate of Sp1 increases appreciably with temperature to reach at 50 °C up to 2 times of that at 25 °C.

These trends of corrosion rate agree with the concept of mixed potential theory. In addition, Table 4 indicates that the corrosion rate of both terminals is increased with the temperature.

Table (4) Corrosion rate of CR specimen couple in different concentrations and temperatures.

CR, gmd				
T, °C	10 ⁻⁵ M CH ₂ O ₂ with 0.1 N NaCl		10 ⁻⁴ M CH ₂ O ₂ with 0.1 N NaCl	
	SP.1 (10 ⁻⁵ M)	SP.2 (0.1 N)	SP.1 (10 ⁻⁴ M)	SP.2 (0.1 N)
25	42.9	8.3	—	—
32	37.1	15.2	74.2	25.6
40	46.3	21.1	—	—
50	84.6	17.3	—	—

3.3 Effect of Aeration on Formic Acid Corrosion in Concentration Cell

Figures (11 to 15) show the results of corrosion potential for two specimens couple of each experiment against time. Experiments were carried out in different acid concentrations aerated solution. From Figures (14 to 18), it is evident that the corrosion potential becomes more positive with adding air bubbles. It is well known that high concentration of O₂ leads to shift the corrosion potential more positive [1, 5, and 16]. Figures (11 through 14) for acid solution at different temperatures indicate that the potential increase associated with air bubbling is high compared to salt solution

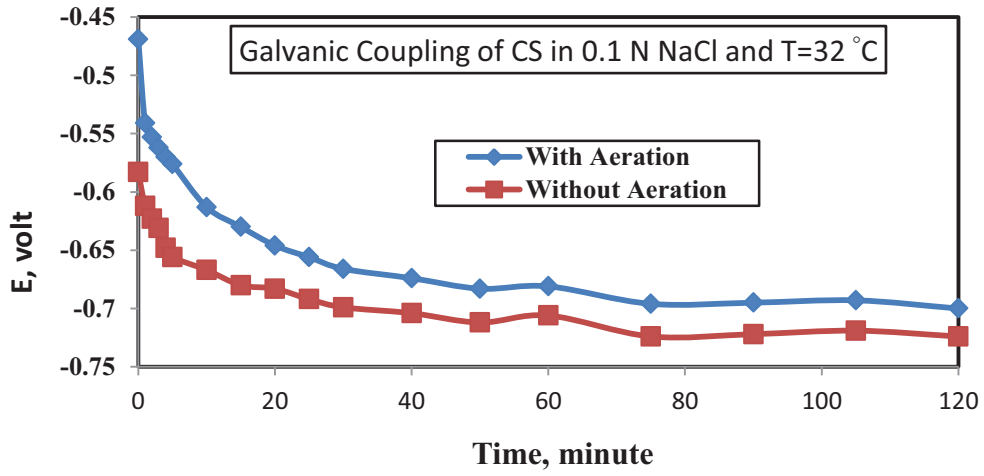


Fig. (11) Corrosion potential vs. time of carbon steel couple in 0.1 N NaCl and T=32 °C.

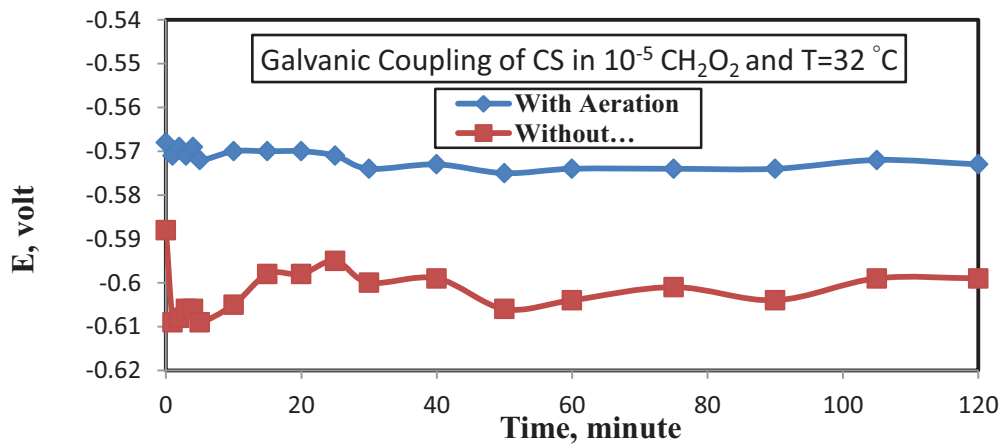


Fig. (12) Corrosion potential vs. time of carbon steel couple in 10⁻⁵ M CH₂O₂ and T=32 °C.

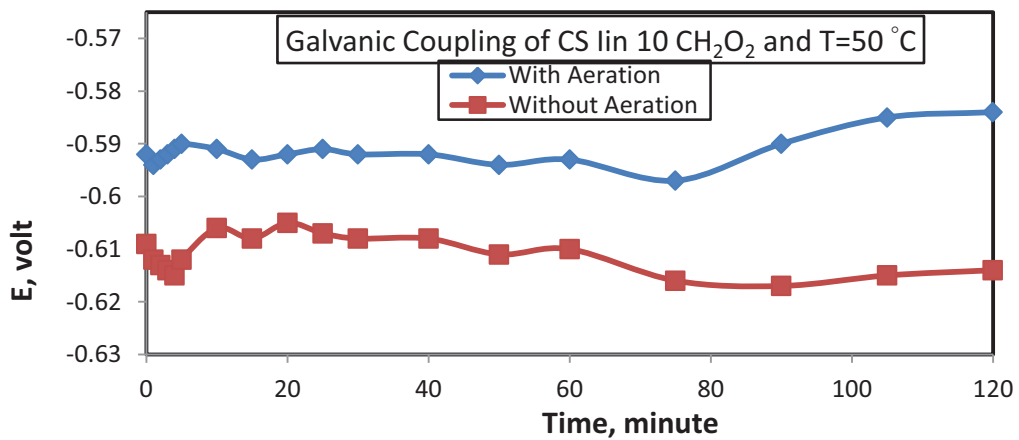


Fig. (13) Corrosion potential vs. time of carbon steel couple in 10⁻⁵ M CH₂O₂ and T=50 °C.

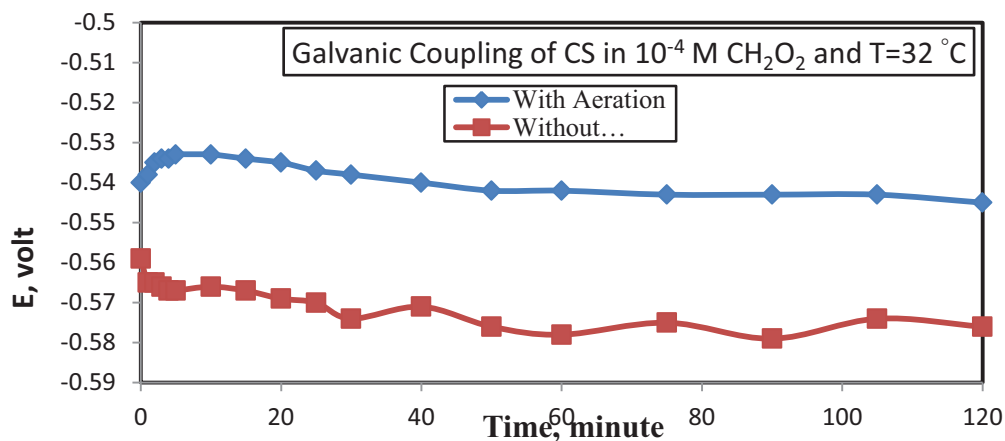


Fig. (14) Corrosion potential vs. time of carbon steel couple in 10^{-4} M CH_2O_2 and $T=32^\circ\text{C}$.

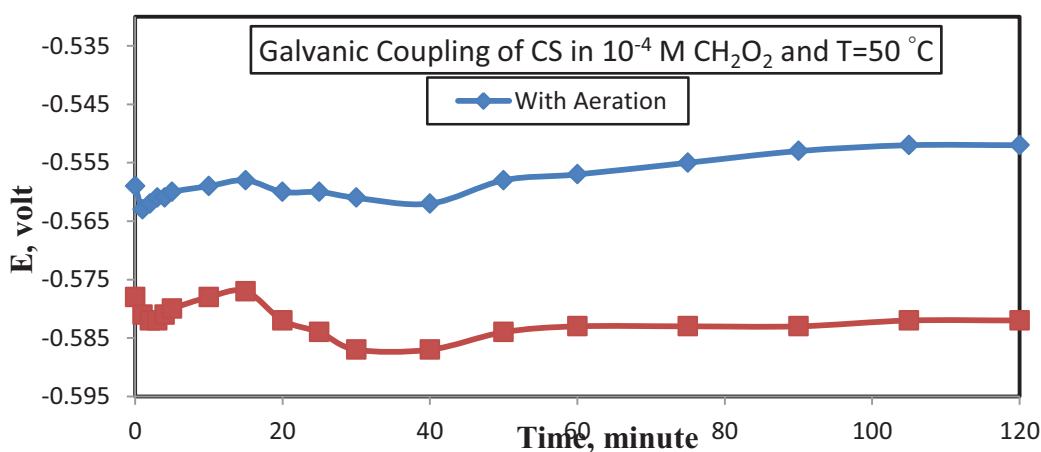


Fig. (15) Corrosion potential vs. time of carbon steel couple in 10^{-4} M CH_2O_2 and $T=50^\circ\text{C}$.

4. Conclusions:

The following conclusions are drawn for the investigated ranges of operating conditions in the current work:

1. The presence of formic acid as a pollutant in water causes a considerable increase in the corrosion rate. When, the concentration reaches 10^{-4} M, the corrosion rate is up to 7.6 times the CR in 0.1N NaCl solution. The potential is shifted to more positive with increasing acid concentration for all temperatures investigated.
2. The concentration cell established by formic acid affects the galvanic corrosion for each terminal. The CS specimen in acid side reaches up to 3 times that in the salt

solution side. When a metal exposed to 0.1N NaCl solution becomes in concentration cell with formic acid, its corrosion rate increases considerably. The percent increase depends on coupled acid concentrations reaching up to 2.3 times when the concentration of formic acid is 10^4 M. In addition, high potential difference is established between the two terminals causing high galvanic current.

3. When air is bubbled in formic acid solution, the O_2 concentration increases causing an appreciable increase in the CR ranging from 2 to 4 times depending on temperature. While in salt solution the CR increases by about 5 % at 32 °C and more than 2.5 times at 50 °C. In addition, the increase in the O_2 concentration shifts potential considerably to more positive direction.
4. Increasing the temperature from 25 °C to 50 °C of 10^{-5} M formic acid solution causes an increase in the galvanic corrosion rate reaches up to 2 times.

Nomenclature

A	Surface Area of Specimen, m^2
CR	Corrosion Rate, $gm/m^2.day$
E	potential, V
t	Time, s
T	Temperature, °C
ΔW	Weight loss, gm

Abbreviations

CS	Carbon Steel
gmd	Gram per Square Meter per Day
SCE	Standard Calomel Electrode
ZRA	Zero Resistance Ammeter
OCP	Open Circuit Potential

References:

1. Revie, R.W. and H. H. Uhlig, *Corrosion and Corrosion Control an Introduction to Corrosion Science and Engineering*”, fourth edition, John Wiley & Sons, Inc., Hoboken New Jersey, 2008.
2. Baboian R., “Material degradation caused by acid rain”, American chemical society, Division of industrial and engineering chemistry, vol. 318, 1986.
3. Simoes, A.M., Bastos A.C., Ferreira M. G., Gonzalez-Garcia Y., Gonzaletz S., Souto R.M., "Use of SVET and SECM to study the galvanic corrosion of an iron–zinc cell", *Corrosion science* 49 (2007) 726-739.
4. Rajeev, P., Surendranathan, A. O. and Murthy, C. S. N. “Corrosion mitigation of the oil well steels using organic inhibitors – A review”, 3(5), pp. 856–869, 2012.
5. Mahato, B. K., C. Y. Cha and W. Shemlit, “Unsteady State Mass Transfer Coefficients Controlling Steel Pipe Corrosion under Isothermal Flow Conditions”, *Corrosion Science*, vol.20, pp.421–441, 1980.
6. Hasan, B. O., "Galvanic corrosion of carbon steel–brass couple in chloride containing water and the effect of different parameters", *Journal of Petroleum Science and Engineering*, 124 (2014)137–14.
7. Hussein, Samar S, B. O. Hasan, Naseer A Al-Haboubi. 2018. “Galvanic Corrosion of Copper / Nickel-Chrome Alloy in an Agitated Sulfuric Acid Solution. *Al-Nahrain Journal for Engineering Sciences (NJES)*, 21(1): 133–140.
8. Cifuentes, L., Electrochemical kinetics helps quantify corrosion phenomena, *J.AntiCorrosion Methods and Materials*, 34(11), 4-9, 1987.
9. Sato, N. (1982) Anodic breakdown of passive films on metals. *J. Electrochem. Soc.*, 129 (2), 255–260.
10. Sato, N. (1990) An Overview on the Passivity of Metals, in *Passivity of Metals Part I, Corrosion Science*, Vol. 31, Pergamon Press, pp. 1–19.
11. Villami, R. F. V., Paola Corio, J. C. Rubim, Silvia M. L. Agostinho. “Effect of sodium dodecylsulfate on copper corrosion in sulfuric acid media in the absence and presence of benzotriazole” *Journal of Electroanalytical Chemistry*, 472 (1999) 112–119.
12. Sato, N. (2001). The stability and breakdown of passive oxide films on metals *J. Indian Chem. Soc.*, 78, 19–26.

13. F. Sense, Oxygen Solubility, North California State, 2001.
14. Shreir L.L, "Corrosion: Metal / Environment Reactions", Newes-Butten Worths, 3rd Ed., Vol.1, (2000).
15. Slaiman, Q. J. M., and Hasan B. O., "Study on Corrosion Rate of Carbon Steel Pipe under Turbulent Flow Conditions" The Canadian Journal of Chemical Engineering, vol. 88, pp. 1114-1120, 2010.
16. Hasan B. O., Sadek S. A., "The effect of temperature and hydrodynamics on carbon steel corrosion and its inhibition in oxygenated acid-salt solution", Journal of Industrial and Engineering Chemistry 20 (2014) 297-307.
17. Osarolube, E., I. O. Owate, N. C. Oforika, "Corrosion Behaviour of Mild and High Carbon Steels in Various Acidic Media", Scientific Research and Essay, No. 6, vol.3, pp. 224-228, 2008.
18. Fontana M.G., "Corrosion Engineering," third edition, McGraw-Hill Book Company, New York, 1986.
19. Hasan B. O., S. A. Sadek, "Corrosion of Carbon Steel in Sodium Sulphate Salt Solution under Flow Conditions" M. Sc. Thesis, Chemical Engineering Department, Al-Nahrain University, December, 2012.
20. Hasan, B. O., Effect of salt content on the corrosion rate of steel pipe in turbulently flowing solutions, Al-Nahrain Journal for Engineering Sciences, 13 (2010) 66-73.
21. Bird R.B., W.E. Stewart, and E.N. Lightfoot, "Transport Phenomena", Second edition, John Wiley and Sons, New York, 2002.
22. Brodkey R. S. and Hershey H. C., "Transport Phenomena", 2nd Printing, Mc Graw Hill, New York, 1989.
23. Slaiman, Q.J.M., B.O. Hasan, H.A Mahmood, Corrosion inhibition of carbon steel under two-phase flow (water-petroleum) simulated by turbulently agitated system, The Canadian Journal of Chemical Engineering 86 (2), 240-248.
24. Hasan, B.O., S.M., Aziz, Corrosion of carbon steel in two phase flow (CO₂ gas-CaCO₃ solution) controlled by sacrificial anode, Journal of Natural Gas Science and Engineering, Journal of Natural Gas Science and Engineering 46 (2017) 71-79.